Low resistance, unannealed, Ohmic contacts to *p*-type In$_{0.27}$Ga$_{0.73}$Sb*

James G. Champlain,[a] Richard Magno, and J. Brad Boos

Naval Research Laboratory, 4555 Overlook Avenue Southwest, Washington, District of Columbia 20375

Unannealed Pd/Pt/Au contacts to *p*-type In$_{0.27}$Ga$_{0.73}$Sb were fabricated and measured. Relatively high hole mobilities, with respect to similarly doped InP-lattice-matched materials, and associated low sheet resistances were measured for the *p*-type In$_{0.27}$Ga$_{0.73}$Sb material. The unannealed Pd/Pt/Au contacts were found to be Ohmic in nature; and for a hole density of 2.9×10^{19} cm^{-3} and a mobility of 160 cm^2/V s, a specific contact resistance of 7.6×10^{-8} Ω cm^2 was measured. [DOI: 10.1116/1.2353838]

I. INTRODUCTION

The 6.1 Å materials, as they are commonly referred to, InAs, AlSb, GaSb, and their alloys (e.g., AlAs$_{0.1}$Sb$_{0.9}$, InAs$_{0.9}$Sb$_{0.1}$), have become highly desirable for use in low-power, high-speed electronic applications due to a large range of available band gaps and band offsets and high electron and hole mobilities. High electron mobility transistors (HEMTs) fabricated from these materials have shown good operating characteristics.[1,2] Recently, the first monolithic microwave integrated circuits fabricated using 6.1 Å based HEMTs have been demonstrated.[3] New materials such as In$_x$Ga$_{1-x}$Sb, InAs$_y$Sb$_{1-y}$, and In$_x$Al$_{1-x}$As$_y$Sb$_{1-y}$, with lattice constants ranging from 6.1 to 6.48 Å, show promise of further power reduction, due greatly to narrower band gaps, while maintaining or possibly improving high-speed operation.[4] Initial work on HEMTs and heterojunction bipolar transistors (HBTs) has been promising. HEMTs have already been demonstrated,[5,6] but the fabrication of HBTs in this material system is relatively new.[7]

A critical aspect of low-power, high-speed HBT operation is a low base resistance and base contact resistance. For example, in order to gain an increase in bandwidth by a factor of δ requires a minimum reduction in base specific contact resistance by a factor of δ^{-2}, in addition to the reduction of various other parasitic elements of the HBT.[8] Previous work on contacts to *p*-type In$_{0.27}$Ga$_{0.73}$Sb examined the thermal stability of Pd-based and Pt-based contacts and the effect of sulfide passivation.[9–11] Specific contact resistances down to 2.8×10^{-7} Ω cm^2 on 1.8×10^{18} cm^{-3} *p*-type In$_{0.27}$Ga$_{0.73}$Sb for unannealed Pd/W/Au contacts were measured.[9] In the article presented here, the electrical characteristics of highly doped *p*-type (Be-doped) In$_{0.27}$Ga$_{0.73}$Sb are examined as related to its application as a base material in 6.2 Å based HBTs. Hall effect measurements in addition to sheet and contact resistance measurements have been performed to evaluate the *p*-type In$_{0.27}$Ga$_{0.73}$Sb material and the quality of unannealed Pd/Pt/Au contacts to it.

II. GROWTH AND FABRICATION

The two samples used for this study were grown by solid-source molecular-beam epitaxy (MBE). The layer structure, designed for Hall effect analysis, consisted from substrate to surface of a semi-insulating (SI) GaAs substrate, a 2 μm undoped AlSb buffer, and a 1 μm Be-doped In$_{0.27}$Ga$_{0.73}$Sb layer. Both samples were grown using this structure, each with a different Be doping level. Measured by Hall effect, the two hole concentrations, and associated hole mobilities, were 1.0×10^{19} cm^{-3} (210 cm^2/V s) and 2.9×10^{19} cm^{-3} (160 cm^2/V s). For the purpose of simplicity, within this article, the 1.0×10^{19} cm^{-3} Hall effect sample will be referred to as sample A and the 2.9×10^{19} cm^{-3} Hall effect sample as sample B.

Figure 1 shows the out of plane x-ray diffraction scan for sample B. Three peaks, associated with the substrate and two grown layers, are evident: the GaAs substrate at 5.653 Å with a full width at half maximum (FWHM) of 28 arc sec, the AlSb buffer at 6.129 Å with a FWHM of 275 arc sec, and the In$_{0.27}$Ga$_{0.73}$Sb layer at 6.206 Å with a FWHM of 580 arc sec. The measured AlSb lattice constant $a_{\text{AlSb,measured}} = 6.129$ Å is slightly smaller than the relaxed AlSb lattice constant $a_{\text{AlSb,relaxed}} = 6.136$ Å due to residual arsenic in the MBE growth system. This low level of residual arsenic produced a light doping of the AlSb buffer with arsenic, resulting in the slight shift in lattice constant of ~0.1% towards GaAs. The broader linewidths of the AlSb and In$_{0.27}$Ga$_{0.73}$Sb x-ray peaks is most likely due to the structural defects induced during epitaxial growth by the large lattice mismatch between the SI GaAs substrate and the AlSb buffer and *p*-type In$_{0.27}$Ga$_{0.73}$Sb layer, respectively.

Transmission line method (TLM) and Hall effect patterns were defined using standard optical lithographic techniques, and Pd/Pt/Au (100/50/1350 Å) contacts were deposited by *e*-beam evaporation. Prior to contact evaporation, a 10 s oxide-removal dip, using a mixture of HCl:H$_2$O (1:10), is performed. A relatively thin contact layer scheme was originally selected to simulate the base contact scheme of a HBT. After initial TLM measurements, additional layers of Ti/Au (50/2450 Å) were deposited to see if the thickness, and thereby resistance, of the metal layers affected the measured sheet and contact resistances. Finally, mesas, to facilitate Hall effect measurements of the *p*-type In$_{0.27}$Ga$_{0.73}$Sb layers,

Report Documentation Page

1. REPORT DATE **AUG 2006**	2. REPORT TYPE	3. DATES COVERED **00-00-2006 to 00-00-2006**

4. TITLE AND SUBTITLE	5a. CONTRACT NUMBER
Low resistance, unannealed, Ohmic contacts to p-type In0.27Ga0.73Sb	5b. GRANT NUMBER
	5c. PROGRAM ELEMENT NUMBER
6. AUTHOR(S)	5d. PROJECT NUMBER
	5e. TASK NUMBER
	5f. WORK UNIT NUMBER

7. PERFORMING ORGANIZATION NAME(S) AND ADDRESS(ES) **Naval Research Laboratory,4555 Overlook Avenue SW,Washington,DC,20375**	8. PERFORMING ORGANIZATION REPORT NUMBER

9. SPONSORING/MONITORING AGENCY NAME(S) AND ADDRESS(ES)	10. SPONSOR/MONITOR'S ACRONYM(S)
	11. SPONSOR/MONITOR'S REPORT NUMBER(S)

12. DISTRIBUTION/AVAILABILITY STATEMENT
Approved for public release; distribution unlimited

13. SUPPLEMENTARY NOTES

14. ABSTRACT

15. SUBJECT TERMS

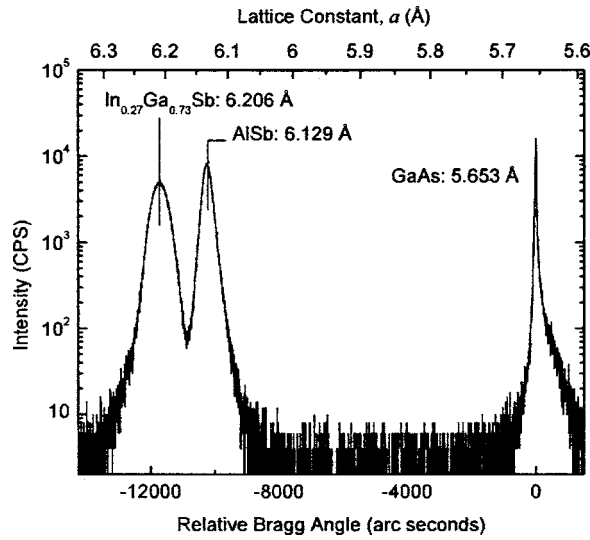| 16. SECURITY CLASSIFICATION OF:			17. LIMITATION OF ABSTRACT	18. NUMBER OF PAGES	19a. NAME OF RESPONSIBLE PERSON
a. REPORT **unclassified**	b. ABSTRACT **unclassified**	c. THIS PAGE **unclassified**	**Same as Report (SAR)**	**3**	

FIG. 1. Out of plane x-ray diffraction scan of sample B ($p=2.9 \times 10^{19}$ cm^{-3}). Three distinct peaks are evident: the GaAs substrate at 5.653 Å with a full width at half maximum (FWHM) of 28 arc sec, the AlSb buffer at 6.129 Å (FWHM of 275 arc sec), and the In$_{0.27}$Ga$_{0.73}$Sb layer at 6.206 Å (FWHM of 580 arc sec).

were etched down to the wide band gap AlSb, using standard optical lithography and phosphoric acid-based etch.

III. MEASUREMENT, RESULTS, AND ANALYSIS

Circular transmission line method (CTLM) patterns were used to evaluate the sheet resistance of the p-type In$_{0.27}$Ga$_{0.73}$Sb material and the contact resistance (and transfer length) associated with the Pd/Pt/Au contacts. The CTLM patterns consisted of an inner contact pad with a radius of 40 μm and a large, outer contact pad with spacings of 4.7, 9.8, 14.5, and 19.7 μm from the inner pads (contact pad sizes and spacings were measured and verified by scanning electron microscope). Measurements were made using a four-point probe setup with a bias current of 10 mA. A two-point probe IV plot of the 4.7 μm spacing from samples A and B demonstrating their Ohmic nature is shown in Fig. 2. The results of the CTLM measurements are shown in Fig. 3. As one can see from Fig. 3, the resistances measured for the thinner Pd/Pt/Au contacts and thicker Pd/Pt/Au/Ti/Au contacts are essentially identical.

The sheet resistances and transfer lengths were determined using the following approximate equation for the resistance of the CTLM patterns:

$$R \approx (R_{\text{sheet}}/2\pi)[\ln(r_o/r_i) + L_T(1/r_o + 1/r_i)], \tag{1}$$

where R is the measured resistance (Ω), R_{sheet} is the sheet resistance (Ω/sq), L_T is the transfer length (μm), r_i is the inner contact pad radius (40 μm, in this case), and r_o is the outer contact pad radius (i.e., the inner contact pad radius r_i plus the relative spacing: 4.7, 9.8, 14.5, or 19.7 μm).[9,12]

The extracted sheet resistance (R_{sheet}) and calculated specific contact resistance (r_C) for sample A ($p=1.0 \times 10^{19}$ cm^{-3}) were 28.8 Ω/sq and 2.8×10^{-7} Ω cm^2, respectively. For sample B ($p=2.9 \times 10^{19}$ cm^{-3}), R_{sheet} and r_C were
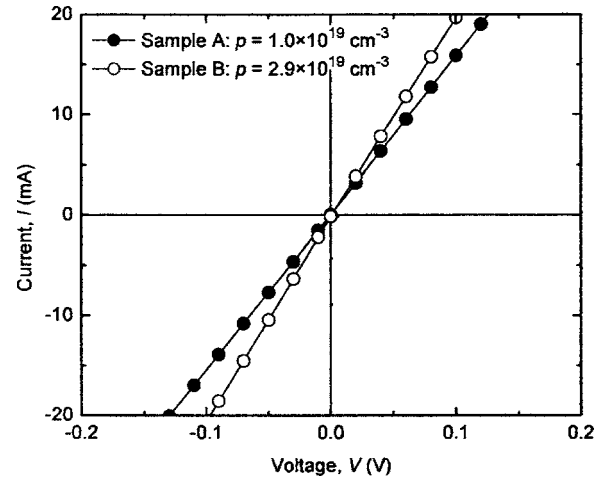

FIG. 2. Two-point probe IV plot of the 4.7 μm spacing from the CTLM patterns from samples A ($p=1.0 \times 10^{19}$ cm^{-3}) and B ($p=2.9 \times 10^{19}$ cm^{-3}).

13.5 Ω/sq and 7.6×10^{-8} Ω cm^2, respectively. The complete results of the Hall effect and the CTLM measurements are summarized in Table I. It should be noted that Eq. (1) is only valid for cases where $4L_T < r_i, r_o$; otherwise, the full equation for the resistance of a CTLM pattern, which involves the use of modified Bessel functions, must be used.[12] In this study, L_T is approximately 40 times smaller than both r_i and r_o, which results in an error of less than 0.1% in the sheet resistance and transfer length extracted using the approximate equation as compared to the full equation.

From Table I, it can be seen that the calculated sheet resistance from the measured Hall effect concentration and mobility agrees quite well with the extracted sheet resistance from the measured CTLM results. Comparing the measured specific contact resistances to those of other state-of-the-art HBT base contact results shows that equivalently low resis-
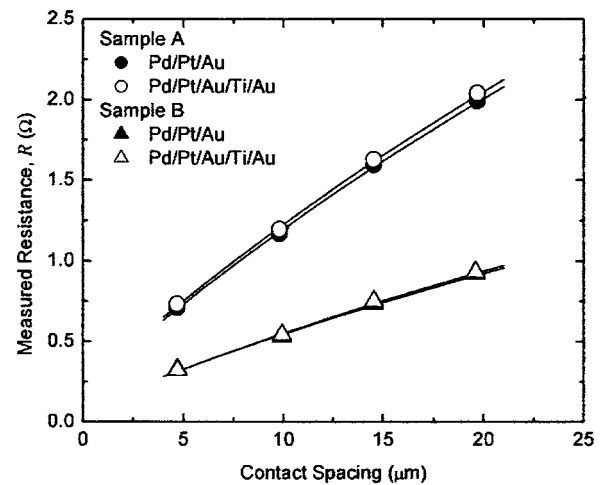

FIG. 3. Plot of measured resistance R vs CTLM contact spacing for both contact metal schemes (Pd/Pt/Au and Pd/Pt/Au/Ti/Au) on samples A ($p=1.0 \times 10^{19}$ cm^{-3}) and B ($p=2.9 \times 10^{19}$ cm^{-3}). The solid lines are the results of fitting Eq. (1) to the measured resistances.

TABLE I. Summary of the Hall effect and circular transmission line method (CTLM) measurements. The calculated R_{sheet} is determined using the results of the Hall effect measurement; the extracted R_{sheet} is found from fitting Eq. (1) to the measured resistance vs CTLM spacing (Fig. 3).

Sample	p (10^9 cm^{-3})	μ (cm^2/V s)	R_{sheet} Calculated (Ω/sq)	R_{sheet} Extracted (Ω/sq)	L_T (μm)	R_C (Ω mm)	r_c (10^{-8} Ω cm^2)
A: Pd/Pt/Au	1.0	210	29.7	28.3	0.95	0.027	26
A: Pd/Pt/Au/Ti/Au	1.0	210	29.7	28.8	0.98	0.028	28
B: Pd/Pt/Au	2.9	160	13.5	13.2	0.82	0.011	8.9
B: Pd/Pt/Au/Ti/Au	2.9	160	13.5	13.5	0.75	0.010	7.6

tances can be achieved with In$_{0.27}$Ga$_{0.73}$Sb and Pd/Pt/Au contacts at relatively lower dopings and without a contact anneal (Fig. 4).

IV. CONCLUSIONS

Low resistance, unannealed, Ohmic Pd/Pt/Au contacts to p-type In$_{0.27}$Ga$_{0.73}$Sb have been demonstrated. Relatively high mobilities, with respect to similarly doped InP-lattice-matched materials, and associated low sheet resistances were measured. For the sample doped at 2.9×10^{19} cm^{-3} (160 cm^2/V s), a specific contact resistance of 7.6×10^{-8} Ω cm^2 for a Pd/Pt/Au/Ti/Au

FIG. 4. Plot of specific contact resistance r_c vs doping concentration (Refs. 9–11 and 13–15).

(100/50/1350/50/2450 Å) contact scheme was measured. To date, this is the lowest measured contact resistance to p-type In$_{0.27}$Ga$_{0.73}$Sb. Compared to other base contact schemes, both annealed and unannealed, from state-of-the-art HBTs, the combination of p-type In$_{0.27}$Ga$_{0.73}$Sb with a Pd/Pt/Au contact shows great promise for high-speed, low-power operation.

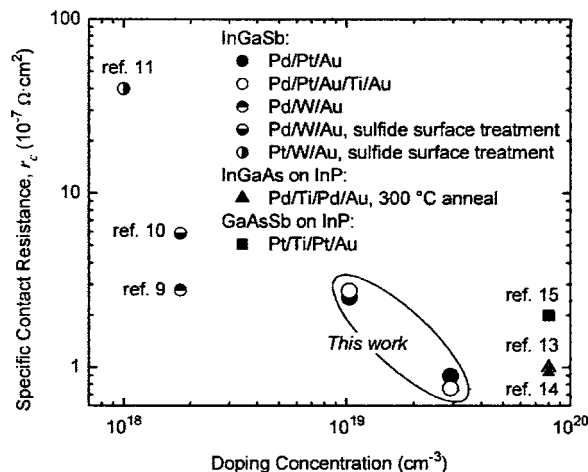[1] J. B. Boos, B. R. Bennett, W. Kruppa, D. Park, J. Mittereder, R. Bass, and M. E. Twigg, J. Vac. Sci. Technol. B **17**, 1022 (1999).
[2] J. B. Boos, B. R. Bennett, W. Kruppa, D. Park, J. Mittereder, W. Chang, and N. H. Turner, Solid-State Electron. **47**, 181 (2003).
[3] W. R. Deal, R. Tsai, M. D. Lange, J. B. Boos, B. R. Bennett, and A. Gutierrez, IEEE Microw. Wirel. Compon. Lett. **15**, 208 (2005).
[4] R. Magno *et al.*, Proceedings of the IEEE Lester Eastman Conference on High Performance Devices, 6–8 August 2002, p. 288.
[5] N. A. Papanicolaou, B. P. Tinkham, J. B. Boos, B. R. Bennett, R. Bass, and D. Park, Proceedings of the 2003 International Semiconductor Device Research Symposium, 10–12 December 2003, p. 352.
[6] W. Kruppa, J. B. Boos, B. R. Bennett, and B. P. Tinkham, Solid-State Electron. **48**, 2078 (2004).
[7] R. Magno *et al.*, Electron. Lett. **41**, 370 (2005).
[8] M. J. W. Rodwell *et al.*, IEEE Trans. Electron Devices **48**, 2606 (2001).
[9] S. H. Wang, S. E. Mohney, and B. A. Hull, J. Vac. Sci. Technol. B **21**, 663 (2003).
[10] S. H. Wang, S. E. Mohney, and J. A. Robinson, Appl. Phys. Lett. **85**, 3471 (2004).
[11] S. H. Wang, J. A. Robinson, and S. E. Mohney, J. Vac. Sci. Technol. A **23**, 293 (2005).
[12] G. S. Marlow and M. B. Das, Solid-State Electron. **25**, 91 (1982).
[13] Z. Griffith, M. Dahlström, M. J. W. Rodwell, X.-M. Fang, D. Lubyshev, Y. Wu, J. M. Fastenau, and W. K. Liu, IEEE Electron Device Lett. **26**, 11 (2005).
[14] M. Dahlström *et al.*, IEEE Electron Device Lett. **24**, 433 (2003).
[15] M. W. Dvorak, C. R. Bolognesi, O. J. Pitts, and S. P. Watkins, IEEE Electron Device Lett. **22**, 361 (2001).